

Direct observation of junction formation in polymer light-emitting electrochemical cells

Jun Gao and Alan J. Heeger

Institute for Polymers and Organic Solids, University of California at Santa Barbara, Santa Barbara, California 93106

I. H. Campbell and D. L. Smith

Los Alamos National Laboratory, Los Alamos, New Mexico 87545

(Received 16 October 1998)

Electroabsorption (EA) measurements are used to determine the electric fields in polymer light-emitting electrochemical cells (LEC's). The EA signals are measured as a function of the dc bias and are found to increase abruptly above a threshold voltage. The EA measurements are compared with the capacitance-voltage and current-voltage characteristics. Calculations using a model based on electrochemical junction formation are in agreement with all of the experimental observations. These results show unambiguously that the picture of electrochemical junction formation in LEC's is correct. [S0163-1829(99)51204-6]

Polymer light-emitting electrochemical cells (LEC's) are a recently invented organic light-emitting device.¹⁻⁸ A LEC consists of a polymer layer, which is a mixture of a luminescent, electronically conducting polymer and an ionically conducting polymer containing an ionic salt (a solid electrolyte), contacted by two metallic electrodes. Polymer LEC's are fundamentally distinct from organic light-emitting diodes (LED's).⁹⁻¹¹ They offer a number of potential advantages over organic LED's including insensitivity to variations in device thickness and to the type of metal used to form the contacts.

The initial papers reporting the invention of LEC's argued that the fundamental operating principle of the device involved the formation of an electrochemical junction.¹⁻⁴ In this picture, the device operates as follows: when the distributions of dissolved salt ions (positive and negative) are spatially separated by a sufficiently large bias, the ions dope the electronically conducting polymer *p* type near the anode and *n* type near the cathode making each region electronically conductive. Thus, an electrochemical junction forms between the *p*-type and *n*-type -doped regions. Electrons injected from the *n*-type side of the junction recombine with holes injected from the *p*-type side of the junction and light is emitted.

Recently, it has been suggested that electrochemical junction formation is not the essential operating principle of a LEC.¹² The operating characteristics of LEC's are attributed to ionic space-charge effects that do not involve electronic doping of the conducting polymer. In this picture, the device operates as follows: the dissolved salt ions accumulate at the contact interfaces under the influence of the applied bias; the accumulation of ions at the contacts makes them Ohmic; the large density of electrons supplied by one contact and of holes supplied by the other contact creates large carrier density gradients inside the device; electrons and holes are driven by diffusion into the center of the device where they recombine and emit light. An essential difference between the two pictures is their contrasting descriptions of the electric fields inside the LEC. In the electrochemical junction picture, there is a large dc electric field in the device after junction formation¹ whereas, in the ionic space-charge pic-

ture, the dc electric field in the device remains small with the applied bias dropping at the contacts.¹²

In this paper, we present electroabsorption (EA) measurements as a function of dc bias at the fundamental and second harmonic of an applied ac bias to determine the electric fields in the LEC. As the dc bias is increased, both the dc and ac electric fields in the cell are found to increase abruptly above a threshold voltage. The increase in the electric fields in the structure is due to the formation of an electrochemical junction. These results are compared with the capacitance and current of the cell, both of which also increase abruptly when the voltage threshold is exceeded. Calculations using a model based on electrochemical junction formation are in agreement with all of the experimental observations. These measurements of the electric fields in LEC's demonstrate unambiguously that the original picture of electrochemical junction formation in these devices is correct.

The electrochemical cells were fabricated using a blend of poly[2-methoxy, 5-(2'-ethyl-hexyloxy)-1,4-phenylene vinylene] (MEH-PPV) and an electrolyte consisting of cis-dicyclohexano-18-crown-6 (CE) and lithium imide (Li imide). The LEC's were fabricated as follows:¹⁻⁸ glass substrates were coated with 15-nm-thick gold films by radio-frequency sputter deposition to serve as a transparent contact; polymer blend layers 260 nm thick (measured by profilometry) were spin cast onto the gold coated substrates from a *p*-xylene solution consisting of MEH-PPV ($M_w = 10^5$), CE, and Li imide in a weight ratio of 4:2:1. Aluminum films 75 nm thick were thermally evaporated onto the polymer layer to serve as a top contact. The aluminum was deposited through a shadow mask to produce cells with active areas of 4×10^{-2} cm². The devices were fabricated and tested in an inert atmosphere at room temperature.

The crown ether/Li-imide electrolyte⁸ was used rather than polyethylene oxide/Li salt^{1,2} in the LEC's because the film optical quality is significantly better (the phase separation occurs on length scales below the wavelength of visible light). The better optical quality is especially important for EA measurements where the signal strength is relatively weak. The LEC's used for these measurements showed typical behavior, including low turn-on voltage and bipolar light emission.

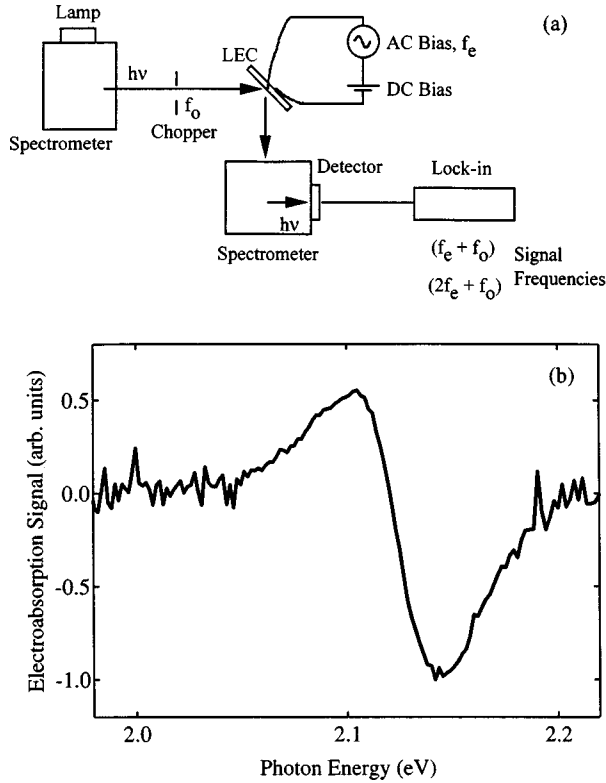


FIG. 1. (a) Schematic illustration of the experimental setup used for the electroabsorption measurements and (b) electroabsorption spectrum from the MEH-PPV in the LEC.

Figure 1(a) shows a schematic of the electroabsorption experiment. A tungsten lamp and a spectrometer were used to select the wavelength of the incident light which was mechanically chopped at frequency f_0 . The incident light passed through the transparent contact and the active layer of the LEC, reflected off the thick top contact, and passed through the active layer and the transparent contact a second time. The reflected light was directed into a second spectrometer and detected using a photodiode. An ac bias (at frequency f_e) and a dc bias were applied to the LEC. For dc voltages both the ions and electrons respond to the applied potential whereas electrons dominate the response to the ac voltage.^{13,14} The signal from the photodiode was measured using a lock-in amplifier. The EA signal at the fundamental frequency of the applied ac bias was detected using the reference frequency $(f_e + f_0)$, and the signal at the second-harmonic frequency was detected using the reference frequency $(2f_e + f_0)$. The modulation of the incident light and the use of an additional spectrometer to filter the reflected light prior to detection were necessary in order to measure the EA signal in the presence of the strong electroluminescence from the LEC.

The EA signal as a function of photon energy is shown in Fig. 1(b). The EA from the MEH-PPV in the active layer of the LEC (Ref. 15) is not significantly effected by the presence of the other components in the mixed layer. The shape of the EA spectrum was found to be independent of both the dc and ac bias applied to the cell. In all of the EA results presented, the incident light was chopped at $f_0 = 330$ Hz, the ac amplitude was 2 V, and the ac bias frequency was 165 Hz when using $(f_e + f_0)$ as a reference and 82.5 Hz when using

$(2f_e + f_0)$ as a reference. The electroabsorption signal was also measured at higher ac bias frequencies, up to 2 KHz. The higher frequency results were similar to the results presented but had lower signal-to-noise ratios.¹⁶ The relatively large bias did not degrade the device during the measurements; EA spectra acquired sequentially over a period of 1 h were equivalent.

The EA signal measured at the two reference frequencies can be used to determine the dc and ac electric fields in the cell. The EA signal from the LEC consists of contributions from the spatially varying electric fields in the LEC integrated across the device. The electroabsorption signal at the fundamental $[E_A(\omega)]$ and second-harmonic frequencies $[E_A(2\omega)]$ of the ac electric field $[E_{ac}(z)\cos(\omega t)]$ in the presence of a dc electric field $[E_{dc}(z)]$ is proportional to the integral (over the thickness of the film) of the square of the total internal electric field. Thus,

$$E_A(\omega) \propto 2 \int_0^L E_{dc}(z) E_{ac}(z) dz, \quad (1a)$$

$$E_A(2\omega) \propto 1/2 \int_0^L [E_{ac}(z)]^2 dz, \quad (1b)$$

where total internal electric field $E(z) = E_{dc}(z) + E_{ac}(z)\cos(\omega t)$, $\omega = 2\pi f_e$, and the integrals are across the LEC of thickness L . If, for simplicity, we consider a bias-dependent region of thickness (d) over which the applied potential is uniformly dropped, the electroabsorption signals are

$$E_A(\omega) \propto [2V_{dc}V_{ac}/d], \quad (2a)$$

$$E_A(2\omega) \propto [1/2(V_{ac})^2/d]. \quad (2b)$$

Thus we expect the EA signals to increase if the region over which the applied potential is dropped decreases due to junction formation in the LEC.

Figure 2(a) shows the measured current density and capacitance as a function of dc bias for the LEC. Both the capacitance and the current density increase dramatically above a threshold voltage. To ensure that the cell was in a steady-state condition, the I - V and C - V characteristics were measured after allowing the cell to equilibrate for 30 sec at each voltage point. Data were acquired with voltage steps of 0.05 V starting at 0 V. The cell capacitance as a function of bias was measured using small signal impedance techniques. A 35 mV amplitude ac signal superimposed on a dc bias was used to measure the cell impedance as a function of ac frequency and dc bias. The capacitance was determined using impedance data in the frequency range from 10–100 kHz.^{13,14} The impedance was least squares fit to a circuit model consisting of a resistor and capacitor in parallel representing the electrochemical cell and a small series resistance representing the doped regions and the thin metal contacts. The zero bias capacitance is the geometric capacitance of the structure. From the polymer film thickness and the zero bias capacitance of these structures, the dielectric constant of the doped polymer blend is found to be about 4.2. The inset in Fig. 2(a) shows the charge separation distance d , derived from the capacitance measurements assuming a parallel plate capacitor model so that $d = \epsilon\epsilon_0/C$, where ϵ is the

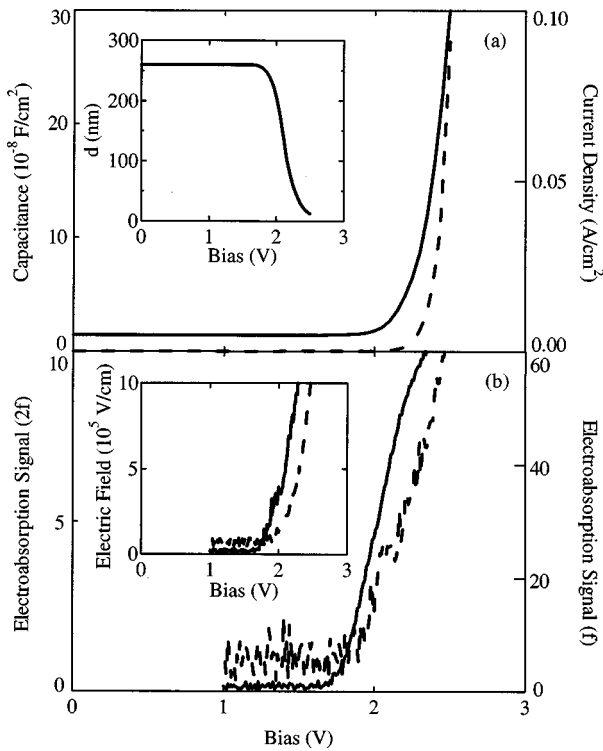


FIG. 2. Experimental results for a 260-nm-thick LEC. (a) Capacitance (solid line) and current density (dashed line) as a function of dc bias. The inset shows the length d derived from the capacitance using a parallel plate model. (b) Electroabsorption signal at the fundamental (solid line) and second-harmonic (dashed line) frequency of the applied ac bias as a function of dc bias. The inset shows the ac (dashed line) and dc (solid line) electric fields calculated using the length derived from the capacitance measurements.

dielectric constant of the doped polymer blend, ϵ_0 is the permittivity of free space, and C is the measured capacitance.

Figure 2(b) shows the EA signals at the fundamental and second-harmonic frequencies of the applied bias as a function of the dc bias. Both EA signals increase sharply at an applied dc bias of about 2 V. The EA signals were measured at the high photon energy peak of the electroabsorption spectrum, at about 2.14 eV [see Fig. 1(b)]. They were acquired with voltage steps of 0.01 V starting at 1 V with a 10 sec delay between each step (below 1 V the signals remain unchanged). The EA signals are normalized to the electroabsorption signal at 2ω and zero dc bias [i.e., at zero bias $E_A(2\omega) = 1$]. At zero bias, the EA signal at 2ω is due to the ac bias voltage being dropped uniformly across the thickness of the LEC. This was verified by measuring the signal from a test film that consisted of the LEC polymer blend without the Li imide salt. This structure behaved as a parallel plate capacitor as determined from impedance measurements. The EA signal from the test structure was equivalent to the signal from the LEC at zero bias. In the inset to Fig. 2(b), we have plotted the electric field in the LEC calculated using the separation distance d obtained from the capacitance and the measured EA signals:

$$E_{dc} = [E_A(\omega)/4] \{G/[2dE_A(2\omega)]\}^{1/2}, \quad (3a)$$

$$E_{ac} = [2GE_A(2\omega)/d]^{1/2}, \quad (3b)$$

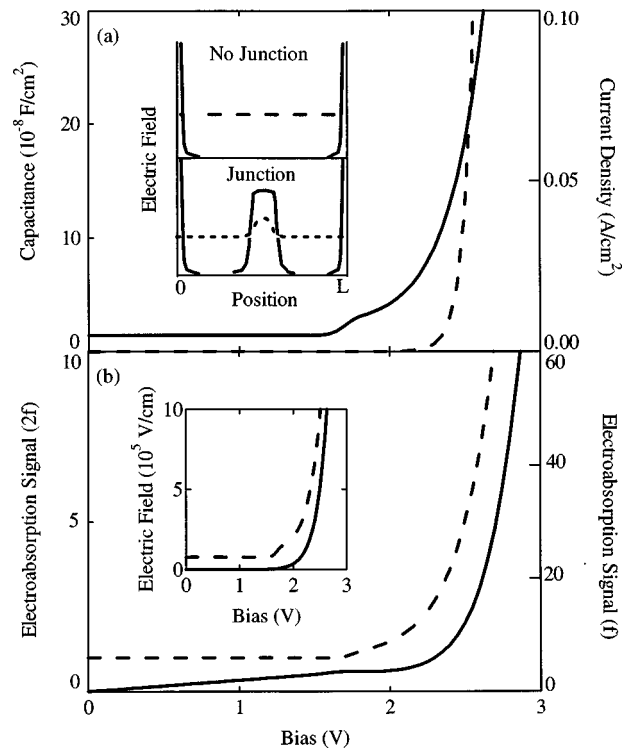


FIG. 3. Device model results for a 260-nm-thick LEC. (a) Capacitance (solid line) and current density (dashed line) as a function of dc bias. The inset shows a schematic illustration of the amplitude of the ac (dashed line) and dc (solid line) electric fields as a function of position in the cell before and after junction formation. (b) Electroabsorption signal at the fundamental (solid line) and second-harmonic (dashed line) frequency of the applied ac bias as a function of dc bias. The inset shows the calculated ac (dashed line) and dc (solid line) electric fields in the junction region.

where G is a constant determined from calibration measurements made on the test layer without salt. Both the dc and ac electric fields increase dramatically and become quite large once the junction is formed above a threshold of about 2 V.

Based on the concept of *in situ* junction formation, a model that describes polymer LEC's has been presented in Ref. 17. Current density, capacitance, the junction width, and the dc potential drop across the junction were calculated within this model. To calculate the EA signals it is also necessary to find the ac field in the junction. In Ref. 17, the increase in the field at the junction center due to an ac bias was evaluated as

$$\frac{dE(W/2)}{dV} = \frac{f(y(0))}{W}, \quad (4)$$

where $E(W/2)$ is the field in the center of the junction, W is the width of the junction, and the function $f(y(0))$ is given in Ref. 17. To calculate the ac electric-field distribution, the cell is approximated as consisting of two distinct regions, inside and outside the junction. The ac electric field is written as $E_{ac}(z) = E_\lambda$ outside the junction region and $E_{ac}(z) = E_\lambda + E_h$ inside the junction region so that $E_\lambda L + E_h W = V_{ac}$. For small ac bias, the increase of the ac field in the junction is taken from Eq. (4)

$$E_h = \frac{f(y(0))}{W} V_{ac}. \quad (5)$$

The electroabsorption signals are then

$$E_A(\omega) \propto 2[E_\lambda(V_{dc} - V_j) + (E_\lambda + E_h)V_j], \quad (6a)$$

$$E_A(2\omega) \propto 1/2[(E_\lambda)^2(L - W) + (E_\lambda + E_h)^2W], \quad (6b)$$

where V_j is the dc potential dropped across the junction.¹⁷ The three important parameters in the model are the energy gap of the electronically conducting polymer, the charge carrier mobility (the model assumes equal electron and hole mobilities), and the salt dissociation free energy. In the calculations presented here, an energy gap of 2.4 eV, a mobility of 10^{-7} cm²/Vs, and a salt dissociation free energy of 0.6 eV were used.^{14,17}

Figure 3(a) shows the calculated current density and capacitance as a function of dc bias for the LEC. The essential features of the calculated current density and capacitance are the same as the measurements; both begin to increase rapidly above a threshold voltage. The absolute values for the calculated capacitance and current density are comparable to those observed experimentally. The insets in Fig. 3(a) show schematic representations of the spatial dependence of the dc (solid line) and ac (dashed line) electric fields in the cell before and after junction formation. Before junction formation there is a dc electric field only in a narrow region near the contacts and the ac electric field is uniform across the bulk of the device. After junction formation there is a dc electric field in the junction region of the device in addition to the thin regions near the contacts and the ac electric field in the junction region is larger than in the remainder of the device.

Figure 3(b) shows the calculated EA signals as a function

of dc bias. The essential features of the calculated EA signals are the same as the measured EA signals shown in Fig. 2(b). Both the calculated and measured EA signals begin to increase rapidly above a threshold voltage. The values of the calculated voltage thresholds are similar to those observed experimentally. The relative magnitudes of the signals (both the experiments and calculations are normalized to the EA signal at 2ω and zero bias) are comparable to those observed experimentally. The inset in Fig. 3(b) shows the calculated ac (dashed line) and dc (solid line) electric fields in the junction region which are similar to the experimental results shown in the inset of Fig. 2(b).

In summary, we presented EA measurements of the electric fields in polymer light-emitting electrochemical cells. The EA signals at the fundamental and second-harmonic frequency of an applied ac bias were used to determine the internal dc and ac electric fields. The EA signals were measured as a function of the dc voltage bias applied to the cell. Both the ac and dc electric field in the cell increase sharply above a threshold voltage as the dc bias is increased. The increase in the electric fields in the structure results from the formation of an electrochemical junction. The EA results are compared with the measured capacitance-voltage and current-voltage characteristics of the cell. Calculations based on a model involving electrochemical junction formation are in agreement with all of the experimental observations. These results show unambiguously that the picture of electrochemical junction formation in these devices is correct.

We thank D. R. Brown for technical support. The work at Los Alamos was partially funded by the Los Alamos National Laboratory LDRD program. The work at UCSB was supported by the National Science Foundation under Grant No. NSF ECE-9528204.

¹Q. B. Pei, G. Yu, C. Zhang, and A. J. Heeger, *Science* **269**, 1086 (1995).

²Q. B. Pei, Y. Yang, G. Yu, C. Zhang, and A. J. Heeger, *J. Am. Chem. Soc.* **118**, 3922 (1996).

³Y. Cao, G. Yu, A. J. Heeger, and C. Y. Yang, *Appl. Phys. Lett.* **68**, 3218 (1996).

⁴Q. B. Pei and Y. Yang, *Synth. Met.* **80**, 131 (1996).

⁵D. J. Dick, A. J. Heeger, Y. Yang, and Q. B. Pei, *Adv. Mater.* **8**, 985 (1996).

⁶Y. Yang and Q. B. Pei, *J. Appl. Phys.* **81**, 3294 (1997).

⁷J. Gao, G. Yu, and A. J. Heeger, *Appl. Phys. Lett.* **71**, 1293 (1997).

⁸Y. Cao, Q. B. Pei, M. R. Anderson, G. Yu, and A. J. Heeger, *J. Electrochem. Soc.* **144**, L317 (1997).

⁹C. W. Tang and S. A. VanSlyke, *Appl. Phys. Lett.* **51**, 913

(1987).

¹⁰N. C. Greenham and R. H. Friend, *Solid State Phys.* **49**, 1 (1995).

¹¹J. R. Sheats, H. Antoniadis, M. Hueschen, W. Leonard, J. Miller, R. Moon, D. Roitman, and A. Stocking, *Science* **273**, 884 (1996).

¹²J. C. deMello, N. Tessler, S. C. Graham, and R. H. Friend, *Phys. Rev. B* **57**, 12 951 (1998).

¹³G. Yu, Y. Cao, and A. J. Heeger, *Appl. Phys. Lett.* **73**, 111 (1998).

¹⁴I. H. Campbell, D. L. Smith, C. J. Neef, and J. P. Ferraris, *Appl. Phys. Lett.* **72**, 2565 (1998).

¹⁵I. H. Campbell, T. W. Hagler, D. L. Smith, and J. P. Ferraris, *Phys. Rev. Lett.* **76**, 1900 (1996).

¹⁶The decreased signal-to-noise ratio was caused by the experimental apparatus, not the performance of the LEC.

¹⁷D. L. Smith, *J. Appl. Phys.* **81**, 2869 (1997).